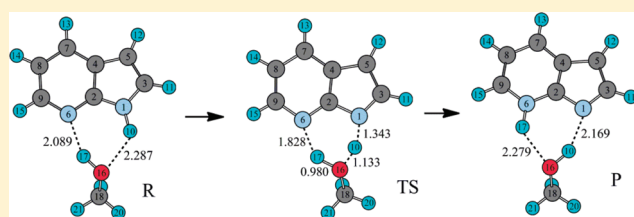


Solvent Effects in the Excited-State Tautomerization of 7-Azaindole: A Theoretical Study

Hua Fang and Yongho Kim*

Department of Applied Chemistry, Kyung Hee University, 1 Seochun-Dong, Giheung-Gu, Yongin-Si, Gyeonggi-Do 446-701, Korea

ABSTRACT: The solvent effect often changes the mechanism of a chemical reaction. Experimental studies of the excited-state tautomerization of 7-azaindole (7AI) suggested that the intrinsic reactions occur via the concerted triple and double proton transfer mechanisms in the gas and liquid phases, respectively. Theoretical study is required to understand how the solvent effect changes the mechanism; however, such studies have rarely been performed in the excited-state. In this study, systematic quantum mechanical calculations were performed to study the excited-state tautomerization of 7AI in methanol. Electronic structures and energies for the reactant, transition state, and product were computed at the complete active space self-consistent field levels with the second-order multireference perturbation theory (MRPT2) to consider the dynamic electron correlation. The IEFPCM and SM8 methods were used to include solvent effect in the excited and ground-state calculations, respectively. The excited-state double proton transfer (ESDPT) in 7AI-CH₃OH and the triple proton transfer (ESTPT) in 7AI-(CH₃OH)₂ both occur via a concerted but asynchronous mechanism. The ESTPT barrier was smaller than the activation energy of solvent reorganization; however, the amount of 7AI-(CH₃OH)₂ in methanol is very small because the complex formation is entropically very unfavorable. Therefore, the ESTPT is not an important path. The MRPT2 barrier of ESDPT was 2.8 kcal/mol, which agrees very well with the experimental value. The MRPT2 barrier of deuterium (D) transfer is larger than the activation energy of solvent reorganization; therefore, the intrinsic D transfer is rate-limiting, while the proton transfer must compete with solvent reorganization. The time-dependent density functional theory (TDDFT) was also used for comparison. Most TDDFT methods used in this study failed to predict transition state structures or barriers of the excited-state tautomerization. Additionally, the TDDFT levels failed to predict correct dipole moments in the excited-state, which produced an unreliable solvent effect on barrier heights.



1. INTRODUCTION

Proton and hydrogen-atom transfer is of key importance to the redox (oxidation–reduction) reactions in many chemical and biological processes, to the proton transport via membrane-spanning proteins, and to the proton relay system in enzymes. In particular, prototropic tautomerisms of DNA base-pairs have attracted much interest for many years^{1–5} since they are related to UV-induced gene mutation. However, it is difficult to monitor the proton transfer in real DNA base pairs because of their conformational complexities and poor spectroscopic properties. Therefore, 7-azaindole (7AI) is utilized as a model compound to mimic the DNA base pair, and the proton transfer in 7AI dimers has been extensively studied. 7AI contains a hydrogen bond donor site (N–H) and an acceptor site (=N–) and displays simple hydrogen-bonding structures upon dimerization and complexation with water and/or alcohols. Proton transfer in the cyclic hydrogen-bonded complexes of amphoteric aromatic molecules with water and/or alcohol, such as 7AI or 7-hydroxyquinoline (7HQ), has also been studied extensively^{6–16} since it can mimic the proton relay system in enzymes and proton transport in membranes.^{17–20} Consequently, a detailed understanding of the multiple proton transfer mechanism at the molecular level might provide insight into these complicated chemical and biological processes.^{21,22}

A large number of proton transfer reactions in hydrogen-bonded complexes of 7AI with water have been studied in the gas phase as well as in the condensed phase.^{23–28} The multiple-proton transfer in 7AI complexes bound to alcohol in the gas phase and in solution was thoroughly studied in order to reveal the proton transfer dynamics in complicated molecular systems such as enzymes and proteins. The ESDPT of a 7AI-CH₃OH complex was observed in the condensed phase, and a two-step model for the tautomerization was proposed.²⁹ In this model, the photoexcited 7AI-CH₃OH undergoes solvent reorganization into the optimal precursor by forming a cyclic hydrogen-bonded complex followed by intrinsic double proton transfer. This model is widely accepted as the mechanism of the excited-state double proton transfer (ESDPT) in 7AI-alcohol complexes in the condensed phase and is also valid for 7HQ-alcohol complexes. The ESDPT of 7AI-CH₃OH in methanol solution was very fast; its time constant was 124 ps at 293 K at an Arrhenius activation energy of 2.32 kJ/mol.²⁹ This activation energy is quite close to the viscosity activation energies of bulk methanol. Moog and Maronchelli²⁹ pointed out that the large-amplitude solvent motion is

Received: September 16, 2011

Revised: November 9, 2011

Published: November 10, 2011

important in the formation of the cyclic conformer; however, such motion could not be entirely rate-limiting because if it were, no kinetic isotope effect (KIE) would be observed. However, the experimental KIE was ~ 3 .²⁹ Those authors also observed that proton transfer rate depends more on the hydrogen-bond donating ability of the solvent than it does on solvent viscosity, and the KIE decreases as the temperature decreases, which support the multistep mechanism of the excited-state tautomerization where no single step is entirely rate-limiting.

Chen et al.³⁰ reported that two protons were involved in the excited-state tautomerization of 7AI in methanol solution based on the proton inventory experiments showing the linear plot of $(k_n/k_0)^{1/2}$ vs n , where k_0 and k_n are tautomerization rate constants in methanol and in a mixture of protiated and deuterated methanol with mole fraction n in CH_3OD , respectively. They also proposed a concerted mechanism for the intrinsic proton transfer step based on the analysis of the rule of geometric mean in KIEs. One of the underlying assumptions in these experiments is that the intrinsic proton (and deuterium) transfer step is rate-limiting, and the force constants of all protons in-flight during the concerted reaction are the same at the transition state (TS). However, this assumption fails when the intrinsic proton transfer step is not rate-limiting or when the multiproton transfer is highly asynchronous so that the force constants of protons in-flight are not the same at the TS.

Very recently, Sekiya et al.^{9,10} have studied the excited-state proton transfer of $7\text{AI}-(\text{CH}_3\text{OH})_n$ ($n = 1-3$) in the gas phase. However, no evidence of tautomer formation has been obtained for $7\text{AI}-(\text{CH}_3\text{OH})_n$ ($n = 1, 3$), except for $7\text{AI}-(\text{CH}_3\text{OH})_2$, which could be attributed to a tautomerization rate too slow to be observed in the visible fluorescence spectrum. In the condensed phase, however, the ESDPT was reported to occur only in $7\text{AI}-\text{CH}_3\text{OH}$ as described above.³⁰ Although the excited-state triple proton transfer (ESTPT) in $7\text{AI}-(\text{CH}_3\text{OH})_2$ occurs in solution, no KIE would be observed if the solvent reorganization is rate-limiting; therefore, it would be difficult to obtain such experimental evidence. Thus, a systematic theoretical study is required to rationalize these results as very few theoretical studies have been performed for the excited-state tautomerization of 7AI in methanol solution.

In the present article, we report high level quantum mechanical data on the tautomerization of the $7\text{AI}-\text{CH}_3\text{OH}$ and $7\text{AI}-(\text{CH}_3\text{OH})_2$ complexes in bulk methanol. The structures and energetics of the reactants, TS, and products were calculated and compared with the experimental results. The complete active space self-consistent field (CASSCF) methods were applied to calculate the structures and energies of the 7AI-methanol complexes. The CASSCF energies were corrected by considering the dynamics electron correlation. The time-dependent density functional theory (TDDFT) has recently been successfully used to study excited-states for many systems; however, most of the studies were focused on the spectroscopic properties. To understand the kinetics and mechanisms of a reaction in the excited-state, detailed information about structures, energies, and vibrational frequencies of reactants and transition states are essential. The TDDFT calculations for excited-state reaction barriers have rarely been performed, particularly for the condensed phase. Thus, there is great interest in determining which functionals are most successful for studying excited-state reactions. In this study, five TDDFT methods, which contained hybrid functional, long-range correction (LC), and empirical dispersion functionals, were used to systematically investigate the excited-state tautomerization reactions in solution.

2. COMPUTATIONAL DETAILS

Reactant, product, and TS geometries of the excited state proton transfer reaction in the $7\text{AI}-(\text{CH}_3\text{OH})_n$ ($n = 1, 2$) complexes were fully optimized at the TDDFT and CASSCF level with 6-31G(d,p), 6-311G(d,p), and 6-311+G(d,p) basis sets using the Gaussian09 program.³¹ At the CASSCF level, the active space, which is an essential component of the calculation, includes four π bonds, four corresponding antibonding orbitals, and one nitrogen lone pair, resulting in an active space of 10 electrons in 9 orbitals, which was denoted as CASSCF(10,9). Vibrational frequencies were also calculated using a similar procedure. Single-point energy calculations were performed using the second-order multireference perturbation theory (MRPT2) for stationary points. All MRPT2 calculations were performed using the GAMESS program.³²

Analytic TDDFT gradients were calculated using the variational TDDFT formulation of Furche and Ahlrichs.³³ Several different exchange-correlation DFT potentials were used in the systems, including Becke's three-parameter Lee–Yang–Parr hybrid functionals (B3LYP),³⁴ Handy and co-workers' long-range corrected version of B3LYP using the Coulomb-attenuating method (CAM-B3LYP),³⁵ long-range-corrected version of BLYP (LC-BLYP),³⁶ hybrid functional of Truhlar and Zhao (M06–2X),³⁷ and the latest functional from Head-Gordon and co-workers, which included empirical dispersion (WB97XD).³⁶ The polarizable continuum model calculations were performed using the integral equation formalism (IEFPCM)^{38–40} at the TDDFT and CASSCF levels to investigate the mechanism of tautomerization in methanol for the excited state. In the IEFPCM calculations, all hydrogen atoms have their individual spheres, and the atomic radii from the UFF force field were scaled by 1.1. The geometries of the reactant, product, and TS were completely optimized in solution. Currently, the solvent effect is not implemented in the MRPT2 calculations. Therefore, the gas phase MRPT2 energies and the solvation energies at the CASSCF level were used to estimate the MRPT2 energies in methanol.

Geometries of the reactants in the $7\text{AI}-(\text{CH}_3\text{OH})_n$ ($n = 1, 2$) complexes in the ground state were also optimized with the M06-2X density functional³⁷ and the 6-31+G(d, p) basis set both in the gas phase and in solution. The solvation effect was predicted using the SM8 model.⁴¹ The SM8 calculations require partial atomic charges, which were obtained using the CM4M charge model. These calculations for solvent effect were carried out using the locally modified Gaussian03⁴² suite of electronic structure programs.^{43,44} The basis set superposition error (BSSE) was corrected for the complex formation energies using the Boys and Bernardi counterpoise correction scheme.⁴⁵ We assumed that the BSSE in the gas phase would be the same as that in solution. In the free energy of solvation, a standard state correction of 1.89 kcal/mol at 298 K was included for transfer from an ideal gas of 1 atm to an ideal solution at a liquid phase concentration of 1 mol L^{−1}.

3. RESULTS AND DISCUSSION

3.1. Ground-State $7\text{AI}-(\text{CH}_3\text{OH})_n$ ($n = 1, 2$) Complexes in Solution. The excited-state prototropic tautomerization for 7AI in bulk solvents^{6,29,46–48} implies that solvation plays a key role in the proton transfer process. The excited-state tautomerization of 7AI in alcohols has been discussed as a two-step process. The first step involves solvent reorganization to form a cyclic

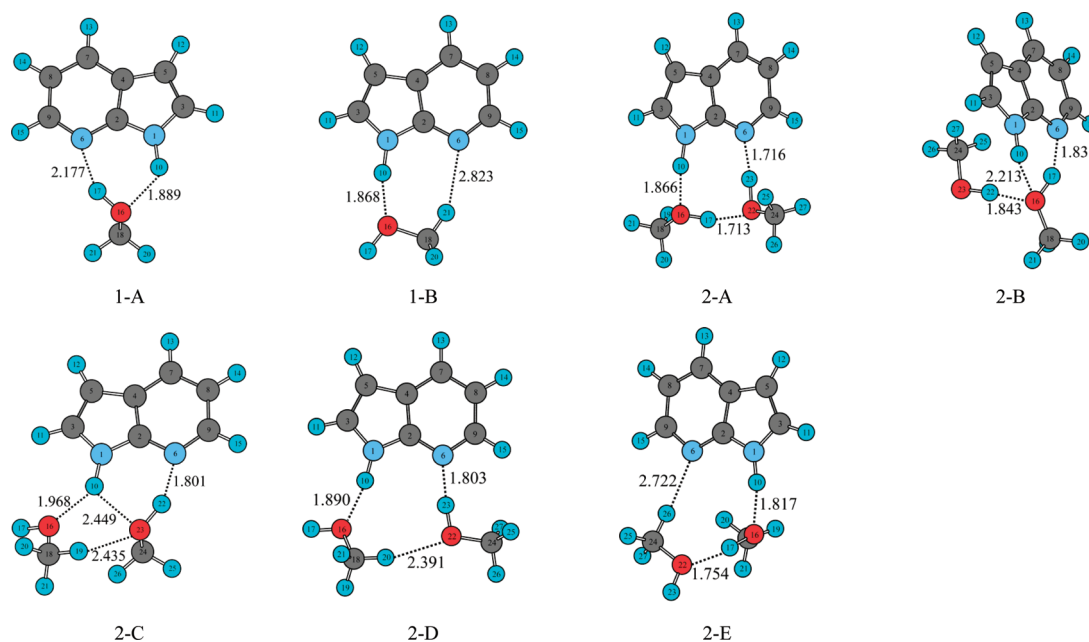
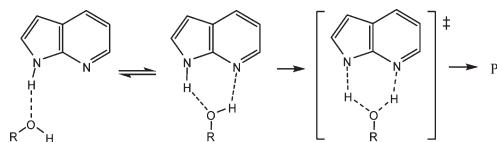


Figure 1. Ground-state H-bonded complexes in the $7\text{AI}-(\text{CH}_3\text{OH})_n$ ($n = 1, 2$) complex in methanol optimized at the M06-2X/SM8/6-31+G(d,p) level.

hydrogen-bonded 7AI-alcohol complex, while the second step is an intrinsic proton transfer.



If the solvent motion was rate-limiting, no significant kinetic isotope effect (KIE) would be expected. However, KIEs for excited-state tautomerization have been observed in 7AI complexes with various alcohols, and Moogs et al.²⁹ suggested that both solvent reorganization and the intrinsic proton transfer step could determine the reaction rate. Since the ESDPT is very fast, the hydrogen-bonded complexes, either cyclic or noncyclic, should be present in solution before the excitation. Therefore, it is necessary to investigate what kind of hydrogen-bonded complex is most likely to be formed in solution. We used the M06-2X method for the liquid-phase calculations, which has been successfully used to reproduce the structures and energies of hydrogen-bonded complexes^{37,49,50} as well as the solvation energies using the SM8 model with class IV charges.⁵¹ The MP2/6-311+G(d,p) level using the IEFPCM was also used for comparison.

Several ground-state conformers of $7\text{AI}-(\text{CH}_3\text{OH})_n$ ($n = 1, 2$) complexes were optimized at the M06-2X/6-31+G(d,p) and MP2/6-311+G(d,p) levels in the gas phase and in methanol, and M06-2X structures in methanol are shown in Figure 1. For $7\text{AI}-\text{CH}_3\text{OH}$, two stable hydrogen-bonded complexes were obtained both in the gas phase and in solution: one with cyclic H-bonds and the other with a single H-bond between the N–H group of 7AI and O in methanol and a weak H-bond between a methyl proton and the pyridinium N of 7AI. The former and later are denoted as 1-A and 1-B, respectively, in the figure. We could not find the 1-B structure without the weak H-bond even in methanol solution. We also tried to find a stable structure with a single

H-bond between OH and the pyridinium N of 7AI; however, no such structure was found because all calculations led to the cyclic 1-A structure shown in Figure 1. For $7\text{AI}-(\text{CH}_3\text{OH})_2$, there are many possible conformers with cyclic or noncyclic H-bonds. Among them, five of the most energy stable complexes, which were denoted as 2-A–2-E, are depicted in Figure 1: 2-A has an eight-membered cyclic H-bonded structure; 2-B has a six-membered cyclic H-bonded structure (similar to 1-A) with an additional H-bond donating CH_3OH ; 2-C has one CH_3OH forming an H-bond from the N–H of 7AI and the other CH_3OH forms a cyclic H-bond similar to that in 1-A; 2-D has two CH_3OH molecules (with a weak H-bond between them), one donating an H-bond to N and the other accepting a bond from the N–H of 7AI; 2-E has one CH_3OH forming an H-bond with the N–H of 7AI and the other forming a bond with CH_3OH .

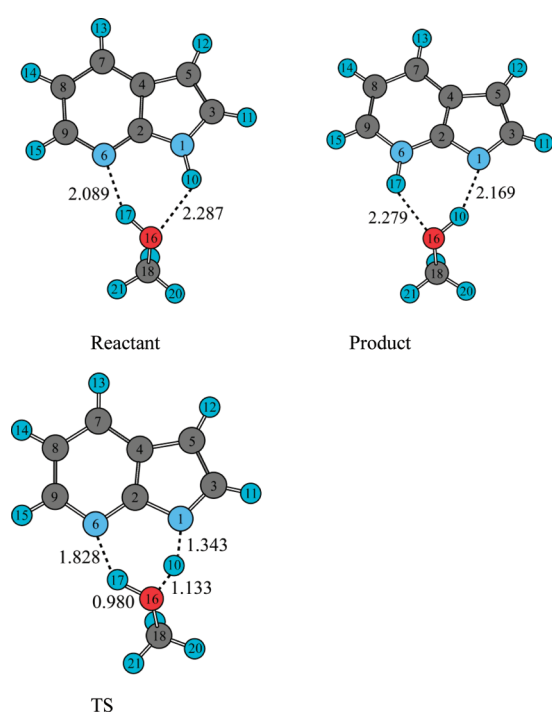
The formation energies of the above conformers in the gas phase and in solution are listed in Table 1. The formation enthalpies (ΔH_{HB}) of 1-B at 0 K are 3.0 and 1.6 kcal/mol higher than those of 1-A at the M06-2X/6-31+G(d,p) level in the gas phase and in methanol, respectively. At the MP2 level, the difference in the ΔH_{HB} value between 1-A and 1-B is 2.8 and 1.3 kcal/mol in the gas phase and in methanol, respectively. These results indicate that 1-A is energetically more stable than 1-B both in the gas phase and in solution. Among the five conformers of $7\text{AI}-(\text{CH}_3\text{OH})_2$, 2-A is energetically most stable both in the gas phase and in solution, and this structure has been confirmed by observing the IR–UV ion-dip spectrum.⁵² For the cyclic $7\text{AI}-\text{CH}_3\text{OH}$ and $7\text{AI}-(\text{CH}_3\text{OH})_2$ conformers (1-A and 2-A), the ΔH_{HB} values at the M06-2X/6-31+G(d,p) level are -9.8 and -20.2 kcal/mol, respectively, in the gas phase, and -3.82 and -9.48 kcal/mol, respectively, in methanol. These results indicate that the latter is energetically more favorable both in the gas phase and in solution.

The predicted formation enthalpies (ΔH_{HB}) and free energies (ΔG) in solution at the two different levels of M06-2X/SM8/6-31+G(d,p) and MP2/IEFPCM/6-311+G(d,p) agree quite well

Table 1. Ground-State Formation Energies (kcal/mol) of Various 7Al-(CH₃OH)_{*n*} (*n* = 1,2) Complexes in the Gas Phase and in Methanol^a

	M06-2X/6-31+G(d,p)			MP2/6-311+G(d,p)		
	ΔE_{HB}	$\Delta H_{\text{HB}}(0\text{ K})$	$\Delta G(298\text{ K})$	ΔE_{HB}	$\Delta H_{\text{HB}}(0\text{ K})$	$\Delta G(298\text{ K})$
1-A	−11.4 (−5.63)	−9.76 (−3.82)	−0.12 (3.86)	−10.2 (−5.50)	−8.45 (−4.08)	1.16 (3.27)
1-B	−7.65 (−4.22)	−6.65 (−2.25)	1.60 (5.02)	−6.89 (−3.80)	−5.62 (−2.83)	3.56 (3.88)
2-A	−23.0 (−13.4)	−20.2 (−9.46)	−2.30 (6.54)	−20.2 (−12.2)	−16.8 (−9.18)	2.46 (6.22)
2-B	−19.1 (−10.3)	−16.2 (−6.43)	2.42 (9.53)	−15.8 (−9.61)	−12.3 (−6.27)	7.51 (9.81)
2-C	−18.0 (−9.93)	−15.4 (−6.79)	4.34 (8.57)	−14.1 (−8.96)	−11.3 (−6.52)	7.16 (8.05)
2-D	−18.0 (−9.85)	−15.4 (−6.81)	4.32 (8.56)	−13.7 (−8.06)	−10.8 (−5.46)	7.59 (8.79)
2-E	−17.0 (−9.56)	−14.3 (−6.49)	4.38 (7.80)	−14.6 (−7.93)	−11.4 (−5.23)	7.66 (9.36)

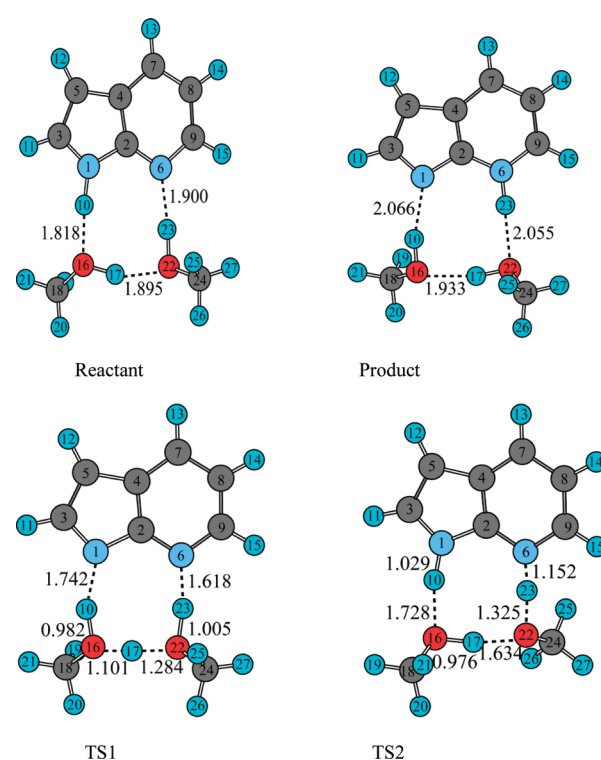
^a Numbers in parentheses are for the methanol solution. The SM8 and IEFPCM methods were used at the M06-2X and MP2 levels, respectively. The structures of 1-A, 1-B, 2-A, 2-B, 2-C, 2-D, and 2-E are shown in Figure 1.

**Figure 2.** Reactant, product, and transition state of the ESDPT in the 7Al-CH₃OH complex in methanol at the CASSCF(10,9)/6-311G(d,p) level.

with each other. In the gas phase, the ΔG values of 1-A and 2-A at the M06-2X level are both negative, and 2-A has a 2.2 kcal/mol smaller value, which suggests that both conformers are present in the gas phase, while 2-A is more preferable. However, in methanol solution, neither complex has negative free energies of formation; 2-A has a 2.7 kcal/mol larger ΔG value than 1-A. The formation of 2-A is entropically very unfavorable even in solution. Therefore, there is no abundance of cyclic H-bonded complexes in solution. Equilibrium constants for the formation of 7Al-CH₃OH can be rewritten as

$$\frac{[7\text{Al} \cdot \text{CH}_3\text{OH}]}{[7\text{Al}]} = K_{\text{eq}}[\text{CH}_3\text{OH}] = f \quad (1)$$

which can be used to estimate the fraction of a cyclic complex in bulk methanol. The fraction of 1-A obtained using the equilibrium constant (from the formation free energy) and the molar

**Figure 3.** Reactant, product, and two transition states (TS1 and TS2) of the ESTPT in the 7Al-(CH₃OH)₂ complex in methanol at the CASSCF(10,9)/6-311G(d,p) level.

concentration of bulk methanol was 0.036, which means that only 3.6% of 1-A is generated in a given methanol solution of 7Al at 298 K. In the 7Al complexes with two CH₃OH groups, only 1% of the composition would be the cyclic 2-A conformer in the ground state. This result agrees very well with the previous Monte Carlo and molecular dynamics studies,^{53,54} which is consistent with the two step model involving the formation of the cyclic complex after excitation. As a result, solvent reorganization plays a very important role in the above process.

Before excitation, most 7Al molecules were assumed to be solvated in a manner that blocks the double proton transfer. However, we were unable to find such complexes in abundance in bulk methanol. Among single-methanol complexes, 1-B blocks the double proton transfer, but its free energies of formation in

Table 2. Selected Bond Distances (Å) of Reactant, Product, and Transition States for the Excited-State Proton Transfer Optimized at the CASSCF(10,9) Level in Methanol^a

	7Al-CH ₃ OH					
	reactant			product		
	r(H ₁₀ –O ₁₆)	r(H ₁₇ –N ₆)		r(N ₁ –H ₁₀)	r(O ₁₆ –H ₁₇)	
6-31G(d,p)	2.261	2.081		2.161	2.257	
6-311G(d,p)	2.287	2.089		2.169	2.279	
	transition state					
	r(N ₁ –H ₁₀)	r(H ₁₀ –O ₁₆)		r(O ₁₆ –H ₁₇)	r(H ₁₇ –N ₆)	
6-31G(d,p)	1.341	1.139		0.990	1.763	
6-311G(d,p)	1.343 (1.299)	1.133 (1.174)		0.980 (1.019)	1.828 (1.605)	
	7Al-(CH ₃ OH) ₂					
	reactant			product		
	r(H ₁₀ –O ₁₆)	r(O ₂₂ –H ₁₇)	r(H ₂₃ –N ₆)	r(N ₁ –H ₁₀)	r(O ₁₆ –H ₁₇)	r(O ₂₂ –H ₂₃)
6-31G(d,p)	1.817	1.874	1.879	2.055	1.920	2.045
6-311G(d,p)	1.818	1.895	1.900	2.066	1.933	2.055
	transition state					
	r(N ₁ –H ₁₀)	r(H ₁₀ –O ₁₆)	r(O ₁₆ –H ₁₇)	r(H ₁₇ –O ₂₂)	r(O ₂₂ –H ₂₃)	r(H ₂₃ –N ₆)
6-31G(d,p)TS1	1.700	0.991	1.087	1.312	1.014	1.593
6-311G(d,p)TS1	1.742 (1.548)	0.982 (1.027)	1.101 (1.045)	1.284 (1.385)	1.005 (1.009)	1.618 (1.599)
6-31G(d,p)TS2	1.031	1.723	0.982	1.614	1.322	1.156
6-311G(d,p)TS2	1.029 (1.067)	1.728 (1.529)	0.976 (1.018)	1.634 (1.451)	1.325 (1.416)	1.152 (1.103)

^a Numbers in parentheses are the bond distances in the gas phase.

solution are larger than that of 1-A. In two-methanol complexes, 2-D and 2-E block the triple proton transfer, but their formation free energies are smaller than that of 2-A. All these complexes are present less abundantly in bulk methanol than 1-A or 2-A. These results suggest that there may be no meaningful H-bonded conformers, which are abundantly present in solution, to block the proton transfer. Before the excitation of 7AI in bulk methanol, the formation of the H-bonded complexes seems to be random and dynamic rather than forming any meaningful equilibrated forms.

3.2. Excited-State Tautomerization of 7AI-(CH₃OH)_n (n = 1, 2) in Solution. 3.2.1. *Structures of Reactants, Products, and Transition States at the CASSCF(10,9) Level.* We preformed IEFPCM calculations for the cyclic reactant, TS, and product at the CASSCF levels to understand the solvent effect in the excited-state tautomerization. The cyclic complexes of reactant, product, and TS in solution were confirmed by frequency calculations. In the excited-state studies, we will discuss only the cyclic conformers of 7AI complexes from now on, so 7AI-CH₃OH and 7AI-(CH₃OH)₂ represent the 1-A and 2-A conformers, respectively, unless mentioned otherwise. The optimized structures of 7AI-CH₃OH and 7AI-(CH₃OH)₂ at the CASSCF(10,9)/6-311G(d,p) level in methanol are depicted in Figures 2 and 3, respectively, and some optimized geometrical parameters of 7AI-CH₃OH and 7AI-(CH₃OH)₂ are listed in Table 2. In the gas phase structure of the 7AI-CH₃OH complex at the CASSCF/6-311G(d,p) level, the H-bond distances of

H₁₀–O₁₆ and N₆–H₁₇ in the reactant and N₁–H₁₀ and O₁₆–H₁₇ in the product were 2.154 and 2.127 Å and 2.199 and 2.187 Å, respectively. In methanol solution, the H₁₀–O₁₆ H-bond in the reactant was 0.133 Å longer and N₆–H₁₇ was 0.038 Å shorter than those in the gas phase. In the 7AI-CH₃OH product, the N₁–H₁₀ and O₁₆–H₁₇ H-bonds became shorter and longer, respectively, in methanol. In other words, H-bonds with a nitrogen atom as an acceptor (N₁–H₁₀ in the product and N₆–H₁₇ in the reactant) shrank in methanol, whereas those with oxygen as an acceptor (H₁₀–O₁₆ in the reactant and O₁₆–H₁₇ in the product) were elongated. These results imply that the solvent effect could increase the excited-state basicity of the nitrogen atom in 7AI to generate slightly shorter and stronger H-bond. The bond distances in the gas phase TSs are also listed in Table 2. Compared to those in the the gas phase structure, the N₁–H₁₀ and N₆–H₁₇ distances were increased in solution, whereas the H₁₀–O₁₆ and O₁₆–H₁₇ distances were decreased, which forms a CH₃OH₂⁺-like moiety in part of the TS. No large changes were observed in the distances depending on the size of the basis sets.

In the reactant and product structures of 7AI-(CH₃OH)₂ at the CASSCF/6-311G(d,p) level, the H-bond distances in solution did not vary much from the corresponding gas phase values. Two TS structures for the ESTPT were found and are shown in Figure 3. In the first TS (denoted as TS1), the H₁₀ moved more than halfway from the N₁ to O₁₆ atom with H₁₇ and H₂₃ barely moving. This generated a CH₃OH₂⁺-like moiety in a portion of the TS (at O₁₆). However, in the second TS (denoted as TS2),

Table 3. Tautomerization Energies, Barrier Heights, and Dipole Moments for the ESPT in 7Al-CH₃OH and 7Al-(CH₃OH)₂ Complexes in Methanol ^a

	ΔV^\ddagger	ΔE_{T}	$\mu(\text{D})$		
			R	TS	P
7Al-CH ₃ OH					
CASSCF(10,9)/6-31G(d,p)	13.0 (10.7) [11.8]	−31.7 (−31.2)	2.38	7.76	2.35
CASSCF(10,9)/6-311G(d,p)	11.6 (9.57) [10.6]	−32.0 (−31.5)	2.33	8.30	2.31
MRPT2/CASSCF(10,9)/6-31G(d,p) ^b	6.43 (4.06) [5.15]	−19.0 (−18.5)			
MRPT2/CASSCF(10,9)/6-311G(d,p) ^b	4.80 (2.78) [3.81]	−18.4 (−17.9)			
7Al-(CH ₃ OH) ₂					
CASSCF(10,9)/6-31G(d,p)	12.5 (9.32) [10.4] ^c	−27.8 (−28.0)	7.43	9.39 ^c	2.43
	11.7 (8.14) [9.26] ^d			10.1 ^d	
CASSCF(10,9)/6-311G(d,p)	12.6 (9.58) [10.7] ^c	−27.1 (−27.3)	7.55	9.77 ^c	2.49
	12.7 (9.07) [10.2] ^d			10.1 ^d	
MRPT2/CASSCF(10,9)/6-31G(d,p) ^b	4.94 (1.81) [2.93] ^c	−15.4 (−15.6)			
	5.34 (1.77) [2.89] ^d				
MRPT2/CASSCF(10,9)/6-311G(d,p) ^b	3.31 (0.27) [1.42] ^c	−14.8 (−15.0)			
	7.05 (3.43) [4.54] ^d				

^a The numbers in parentheses and brackets are the barrier heights of H and D transfers including zero-point energies, respectively. Energies are in kcal/mol. ^b The energy includes nonelectrostatic terms. ^c TS1. ^d TS2.

Table 4. Selected Bond Distances (Å) of Reactant, Product, and Transition States for the Excited-State Proton Transfer in 7Al-CH₃OH Calculated at the TDDFT Levels in Methanol

computational method	reactant		product	
	$r(\text{H}_{10}-\text{O}_{16})$	$r(\text{H}_{17}-\text{N}_6)$	$r(\text{N}_1-\text{H}_{10})$	$r(\text{O}_{16}-\text{H}_{17})$
B3LYP/6-31G(d,p)	1.939	1.809	1.933	2.049
B3LYP/6-311+G(d,p)	2.013	1.851	1.954	2.130
CAM-B3LYP/6-31G(d,p)	1.908	1.807	1.922	2.003
CAM-B3LYP/6-311+G(d,p)	1.971	1.850	1.945	2.058
LC-BLYP/6-31G(d,p)	1.884	1.798	1.900	1.950
LC-BLYP/6-311+G(d,p)	1.938	1.833	1.917	1.990
M06-2X/6-31G(d,p)	1.943	1.824	1.982	2.025
M06-2X/6-311+G(d,p)	2.010	1.870	1.984	2.100
WB97XD/6-31G(d,p)	1.933	1.836	1.949	2.022
WB97XD/6-311+G(d,p)	2.015	1.854	1.948	2.116
computational method	transition state			
	$r(\text{N}_1-\text{H}_{10})$	$r(\text{H}_{10}-\text{O}_{16})$	$r(\text{O}_{16}-\text{H}_{17})$	$r(\text{H}_{17}-\text{N}_6)$
B3LYP/6-31G(d,p)	1.260	1.253	1.153	1.376
B3LYP/6-311+G(d,p)	1.310	1.201	1.117	1.434
CAM-B3LYP/6-31G(d,p)	1.277	1.224	1.121	1.412
CAM-B3LYP/6-311+G(d,p)	1.329	1.175	1.091	1.473
LC-BLYP/6-31G(d,p)	1.286	1.208	1.114	1.415
LC-BLYP/6-311+G(d,p)	1.332	1.167	1.093	1.460
M06-2X/6-31G(d,p)	1.282	1.218	1.094	1.458
M06-2X/6-311+G(d,p)	1.320	1.180	1.071	1.511
WB97XD/6-31G(d,p)	1.289	1.208	1.111	1.424
WB97XD/6-311+G(d,p)	1.342	1.159	1.079	1.490

the H₂₃ moved more than halfway from the O₂₂ to the N₆ atom, but H₁₀ and H₁₇ barely moved, resulting in a CH₃O[−]-like moiety in a part of the TS (at O₂₂). Two TSs of the concerted but highly asynchronous multiproton transfer in 7Al-(H₂O)₂ were previously

observed both in the gas phase and in water.²⁸ The methanol complex showed similar behavior in the ESTPT. Considering only one proton migrated substantially, while the other two barely moved, a stepwise mechanism with a possible intermediate was

Table 5. Selected Bond Distances (Å) of Reactant, Product, and Transition States for the Excited-State Proton Transfer in 7AI-(CH₃OH)₂ Calculated at the TDDFT Levels in Methanol

computational method	reactant			product		
	r(H ₁₀ –O ₁₆)	r(O ₂₂ –H ₁₇)	r(H ₂₃ –N ₆)	r(N ₁ –H ₁₀)	r(O ₁₆ –H ₁₇)	r(O ₂₂ –H ₂₃)
B3LYP/6-31G(d,p)	1.690	1.674	1.679	1.806	1.729	1.827
B3LYP/6-311+G(d,p)	1.733	1.727	1.729	1.834	1.770	1.866
CAM-B3LYP/6-31G(d,p)	1.664	1.649	1.675	1.794	1.702	1.795
CAM-B3LYP/6-311+G(d,p)	1.709	1.700	1.724	1.818	1.738	1.827
LC-BLYP/6-31G(d,p)	1.638	1.613	1.661	1.766	1.661	1.749
LC-BLYP/6-311+G(d,p)	1.685	1.662	1.705	1.783	1.692	1.778
M06-2X/6-31G(d,p)	1.650	1.668	1.662	1.845	1.754	1.821
M06-2X/6-311+G(d,p)	1.704	1.721	1.719	1.862	1.812	1.863
WB97XD/6-31G(d,p)	1.695	1.704	1.705	1.826	1.751	1.816
WB97XD/6-311+G(d,p)	1.717	1.726	1.728	1.817	1.762	1.823

computational method	transition state					
	r(N ₁ –H ₁₀)	r(H ₁₀ –O ₁₆)	r(O ₁₆ –H ₁₇)	r(H ₁₇ –O ₂₂)	r(O ₂₂ –H ₂₃)	r(H ₂₃ –N ₆)
B3LYP/6-31G(d,p)	1.118	1.447	1.104	1.341	1.349	1.164
B3LYP/6-311+G(d,p)	1.094	1.508	1.094	1.356	1.477	1.103
CAM-B3LYP/6-31G(d,p)	1.139	1.388	1.109	1.315	1.295	1.193
CAM-B3LYP/6-311+G(d,p)TS1	1.382	1.124	1.122	1.296	1.097	1.428
CAM-B3LYP/6-311+G(d,p)TS2	1.105	1.465	1.097	1.334	1.435	1.115
LC-BLYP/6-31G(d,p)	1.251	1.222	1.129	1.271	1.159	1.319
LC-BLYP/6-311+G(d,p)	1.370	1.127	1.130	1.275	1.100	1.415
M06-2X/6-31G(d,p)	1.244	1.233	1.106	1.310	1.106	1.398
M06-2X/6-311+G(d,p)	1.375	1.125	1.106	1.317	1.075	1.462
WB97XD/6-31G(d,p)	1.131	1.402	1.104	1.323	1.341	1.158
WB97XD/6-311+G(d,p)TS1	1.411	1.101	1.119	1.297	1.083	1.445
WB97XD/6-311+G(d,p)TS2	1.108	1.452	1.103	1.320	1.463	1.101

expected. However, all calculations to find this intermediate in methanol led to either the reactant or the product. Thus, these results suggest that there are potentially two concerted but asynchronous processes in the ESTPT. The solvent effect increased the N₁–H₁₀ and N₆–H₂₃ distances of TS1 and reduced the O₁₆–O₂₃ distance by slightly moving H₁₇ toward the center of two oxygen atoms to form a short and strong H-bond, which resulted in the larger ion-pair character of TS. In TS2, the O₁₆–H₁₀ and O₂₂–H₁₇ distances were increased in solution, but the O₂₂–H₂₃ increased slightly, which probably increased the partial charge density of the CH₃O[−]-like moiety in a part of the TS.

3.2.2. Energetics and Mechanism of the Excited-State Tautomerization in Solution. Barrier heights (ΔV^\ddagger), excited-state tautomerization energies (ΔE_T), and dipole moments (μ) for the 7AI-CH₃OH and 7AI-(CH₃OH)₂ complexes are listed in Table 3. Tautomerization energies and barrier heights were highly dependent on the dynamic electron correlation. The MRPT2 level predicted somewhat different tautomerization energies for 7AI-CH₃OH and 7AI-(CH₃OH)₂ in methanol; the tautomerization of 7AI-CH₃OH was more exoergic than that of 7AI-(CH₃OH)₂. The ZPE-corrected ΔE_T value of 7AI-CH₃OH was 2.9 kcal/mol lower than that of 7AI-(CH₃OH)₂ at the MRPT2 level using the 6-311G(d,p) basis sets, which means that the tautomerization of 7AI-(CH₃OH)₂ is thermodynamically less favorable in methanol.

The ΔV^\ddagger values greatly depend on the dynamic electron correlation. In particular, the relative ΔV^\ddagger values of TS1 and

TS2 in 7AI-(CH₃OH)₂ would not be correctly predicted unless the dynamic electron correlation with sufficiently large basis sets was used. The ZPE-corrected ΔV^\ddagger value of 7AI-CH₃OH was only 2.8 kcal/mol at the MRPT2/6-311G(d,p) level in methanol. The activation energy of the solvent viscosity was 2.6 kcal/mol for methanol,²⁹ which is nearly the same as the ΔV^\ddagger value. This result suggests that the ESDPT is possible in solution at room temperature, while no tautomerization was observed in the gas phase, which is consistent with the experimental results. In the ESTPT of the 7AI-(CH₃OH)₂ complex, the ZPE-corrected ΔV^\ddagger value of TS1 was 0.3 kcal/mol, which is 3.2 kcal/mol lower than that of TS2. This indicates that the ESTPT would occur preferably via TS1. The ZPE-corrected ΔV^\ddagger value of 7AI-(CH₃OH)₂ was 2.5 kcal/mol lower than that of 7AI-CH₃OH, which suggests that the ESTPT is approximately 70 times faster than the ESDPT in methanol without considering the tunneling effect.

No experimental studies have reported the possibility of the ESTPT by forming cyclic H-bonded complexes with two CH₃OH molecules in methanol. Proton inventory experiments showing the linear plot of $(k_n/k_0)^{1/2}$ vs n and the RGM in KIEs were used as evidence for the concerted two proton mechanism in the intrinsic proton transfer step by forming cyclic 7AI-CH₃OH.³⁰ The underlying assumption of the above experiments is that the force constants of the two protons in the concerted rate-limiting step are the same at the TS. However, this assumption fails when the multiproton transfer is highly asynchronous

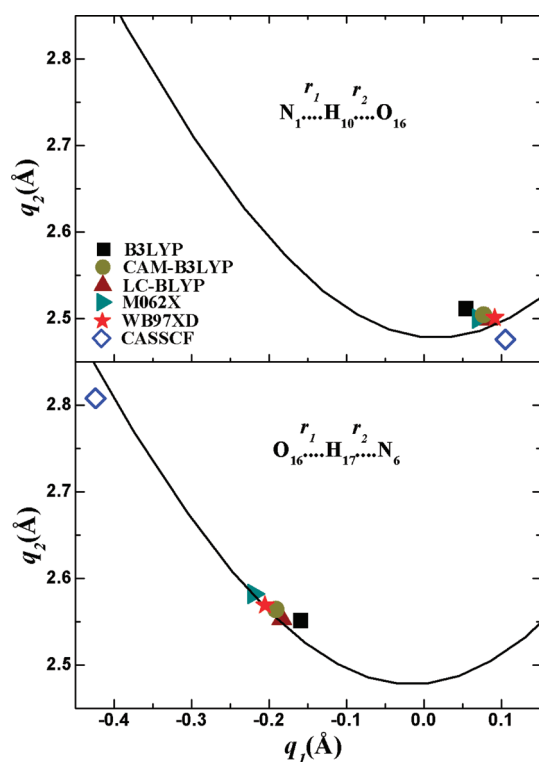


Figure 4. Correlation of the H-bond distances $q_2 = r_1 + r_2$ with the proton transfer coordinate $q_1 = (1/2)(r_1 - r_2)$ for the 7AI-CH₃OH complex in methanol. All points are for the transition states in S_1 optimized at the CASSCF/6-311G(d,p) and TDDFT/6-311+G(d,p) levels in solution. The solid lines designate the correlation that satisfies the conservation of the bond order.

and/or the intrinsic proton transfer is not rate-limiting. Although the ESTPT in 7AI-(CH₃OH)₂ occurs in solution, no KIE is observed if solvent reorganization is rate-limiting. In addition, the amount of ground-state 7AI-(CH₃OH)₂ before excitation is very small in methanol. These results suggest that 7AI-CH₃OH is generated in a larger quantity in the ground state than 7AI-(CH₃OH)₂, although the ESTPT in 7AI-(CH₃OH)₂ occurs faster than the ESDPT in 7AI-CH₃OH; therefore, the tautomerization path of the ESTPT seems to be unimportant. Moreover, the ΔV^\ddagger value of ESTPT via TS1 is lower than the activation energy of methanol viscosity; therefore, the tautomerization of 7AI-(CH₃OH)₂ must be limited by solvent reorganization.

The experimental Arrhenius activation energy of the excited-state tautomerization was 2.3 kcal/mol in methanol,²⁹ which is somewhat smaller than the ΔV^\ddagger value of 7AI-CH₃OH. Considering the lack of tunneling effect in this study and the kinetics were mixed with solvent reorganization, the agreement between theory and experiment is quite good. The barrier heights of deuterium (D) transfer are also listed in Table 3. The ΔV^\ddagger value of D transfer in 7AI-CH₃OH at the MRPT2 level using the 6-311G(d,p) basis set is 3.81 kcal/mol, which is 1.03 kcal/mol larger than that of the proton (H) transfer. The KIE estimated using these values without considering the tunneling effect is 5.87, which is larger than the experimental values. This value of KIE would be obtained only if H and D transfers were both rate-limiting. The smaller KIE value might be attributed to the slower H transfer rate that is limited by the solvent reorganization. This result also suggests that the intrinsic H transfer is not entirely

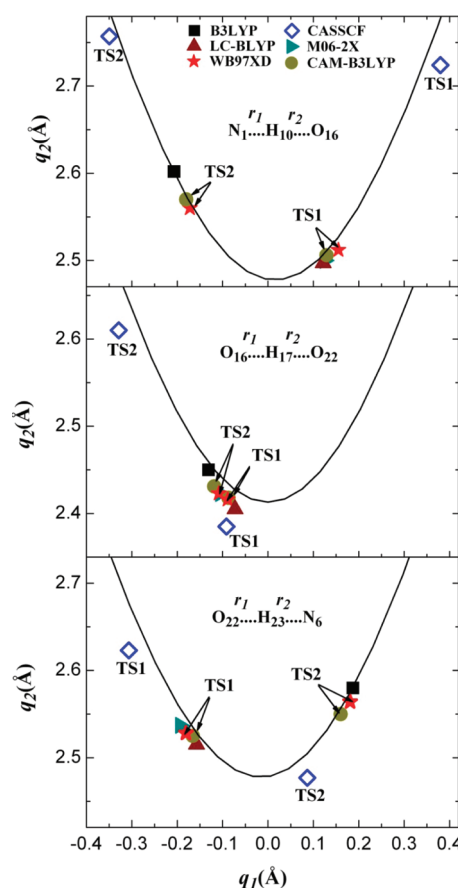


Figure 5. Correlation of the H-bond distances $q_2 = r_1 + r_2$ with the proton transfer coordinate $q_1 = (1/2)(r_1 - r_2)$ for the 7AI-(CH₃OH)₂ complex in methanol. All points are for the transition states in S_1 optimized at the CASSCF/6-311G(d,p) and TDDFT/6-311+G(d,p) levels in solution. The solid lines designate the correlation that satisfies the conservation of the bond order.

rate-limiting (must be competing with solvent reorganization) in the excited-state tautomerization. The ΔV^\ddagger value of D transfer is larger than the activation energy of methanol viscosity; therefore, the intrinsic D transfer is rate-limiting. However, in the 7AI-(CH₃OH)₂ complex, the ΔV^\ddagger value of D transfer is smaller than the activation energy of methanol viscosity; therefore, the solvent reorganization is still rate-limiting in this case.

3.2.3. Structures and Energetics at the TDDFT Level. In order to investigate which functionals are most successful for studying excited-state reactions, we tested five TDDFT methods, namely, B3LYP, CAM-B3LYP, LC-BLYP, M06-2X, and WB97XD. Geometric parameters of reactant, product, and transition states for 7AI-CH₃OH and 7AI-(CH₃OH)₂ calculated at the TDDFT levels in methanol are listed in Tables 4 and 5, respectively. In order to explain kinetic properties, it is very important to correctly calculate the TS structure. In the TS, the ESDPT/ESTPT occurred in a concerted but asynchronous way. Limbach et al.^{55–57} defined the hydrogen bond coordinates $q_1 = (1/2)(r_{AH} - r_{BH})$ and $q_2 = r_{AH} + r_{BH}$ to represent the correlation between r_{AH} and r_{BH} in many hydrogen-bonded complexes (A–H···B), which can be used to study the characteristics of TS, such as earliness or lateness, tightness or looseness, bond order, and asynchronicity. For a linear H-bond, q_1 represents the distance of H from the H-bond center, and q_2 represents the

Table 6. Tautomerization Energies, Barrier Heights, and Dipole Moments for the ESPT in 7AI-CH₃OH and 7AI-(CH₃OH)₂ Calculated at the TDDFT Levels in Solution^a

computational method	7Al-CH ₃ OH					7Al-(CH ₃ OH) ₂				
	ΔV^\ddagger	ΔE_T	$\mu(D)$			ΔV^\ddagger	ΔE_T	$\mu(D)$		
			R	TS	P			R	TS	P
B3LYP/6-31G(d,p)	8.79 (4.23)	−15.5 (−15.1)	5.89	4.01	2.09	5.16 (0.46)	−13.4 (−12.7)	5.30	6.82	2.11
CAM-B3LYP/6-31G(d,p)	8.33 (4.13)	−16.2 (−15.6)	5.42	4.30	2.18	5.11 (−0.09)	−14.0 (−13.1)	4.87	5.90	2.43
LC-BLYP/6-31G(d,p)	8.04 (4.08)	−14.9 (−14.2)	4.61	4.12	2.27	4.50 (−1.38)	−12.7 (−11.7)	3.95	3.87	2.66
M06-2X/6-31G(d,p)	7.04 (3.47)	−16.8 (−16.1)	5.73	4.51	2.30	3.23 (−1.38)	−14.3 (−13.5)	5.19	4.75	3.07
WB97XD/6-31G(d,p)	9.77 (5.59)	−16.4 (−15.9)	5.64	4.39	2.30	6.59 (1.48)	−14.2 (−13.3)	5.15	6.62	3.02
B3LYP/6-311+G(d,p)	11.7 (7.54)	−13.7 (−13.4)	5.93	4.54	2.11	6.77 (3.11)	−12.1 (−11.6)	5.46	8.21	1.91
CAM-B3LYP/6-311+G(d,p)	11.7 (8.01)	−13.2 (−12.6)	5.27	4.95	2.22	8.80 (3.61) ^b	−11.7 (−11.0)	4.88	5.47 ^b	2.24
						7.51 (3.47) ^c			7.46 ^c	
LC-BLYP/6-311+G(d,p)	11.7 (8.13)	−10.9 (−10.2)	4.44	4.75	2.33	8.26 (3.08)	−9.51 (−8.73)	4.04	5.07	2.45
M06-2X/6-311+G(d,p)	9.89 (6.53)	−13.7 (−13.1)	5.73	5.10	2.59	5.61 (1.71)	−12.2 (−11.1)	5.12	5.49	3.06
WB97XD/6-311+G(d,p)	12.6 (9.16)	−13.4 (−12.8)	5.60	5.11	2.59	9.77 (4.85) ^b	−11.8 (−10.9)	5.10	5.73 ^b	2.35
						8.46 (4.38) ^c			7.74 ^c	

^a The numbers in parentheses include zero-point energies. Energies are in kcal/mol. ^b TS1. ^c TS2.

distance between atoms A and B. The negative or positive q_1 value corresponds to early or late TS, respectively, and the small or large q_2 value corresponds to tight or loose TS, respectively. In addition, the two q_1 values at the TS of double proton transfer should be very similar and different in the synchronous and asynchronous mechanisms, respectively. Bond distance depends on bond energy and bond order. In the A–H···B complexes, the r_{AH} and r_{BH} distances depend on each other, leading to allowed r_{AH} and r_{BH} values based on the Pauling equations under the assumption that the sum of the two bond orders is conserved. This type of correlation, i.e., the bond energy bond order method, has been used for many years to study hydrogen atom transfer.^{58,59} When H is transferred from A to B in the A–H···B complex, q_1 increases from a negative to positive value, and q_2 goes through a minimum at $q_1 = 0$. Limbach et al.^{55–57} suggested that both proton transfer and hydrogen-bonding coordinates could be combined into the same correlation.

The correlation between q_1 and q_2 at the TS of 7AI-CH₃OH and 7AI-(CH₃OH)₂ in methanol are illustrated in Figures 4 and 5. Interestingly, all correlation points of TS were at or near the solid lines that satisfy the Pauling equations, although their geometric parameters highly depend on the theoretical level. The parameters for the Pauling equations were taken from the literature.⁵⁶ At the TS of 7AI-CH₃OH, the correlation of q_1 with q_2 was dependent on the solvent effect, which greatly enhanced the asynchronicity of the double proton transfer; the differences in q_1 values between H₁₀ and H₁₇ increased significantly. At the TDDFT levels, the positive and negative q_1 values of H₁₀ and H₁₇, respectively, suggested asynchronous double proton transfer, where the H₁₀ atom moved first, followed by the H₁₇ atom. The TDDFT level generated the same mechanism (but with significantly smaller asynchronicity) as the CASSCF. For the TS of 7AI-(CH₃OH)₂ at the CASSCF level, as described above, two TS structures represent two different ESTPT mechanisms. At TS1, the H₁₀ and H₂₃ correlation points appeared in the right and left side of Figure 5, respectively, which showed large asynchronicity of TS1, i.e., the TS positions in terms of the H₁₀ and H₂₃ transfers became very late (product-like) and early (reactant-like), respectively. At TS2, however, the H₁₀ and H₂₃ correlation points

appeared in the opposite manner. At the TDDFT levels, two TSs (TS1 and TS2) were obtained only at the CAM-B3LYP/6-311+G(d,p) and WB97XD/6-311+G(d,p) levels. As shown in Figure 5, the correlation points of TS1 for H₁₀ transfer and H₂₃ transfer at these two levels are not separated as much as those at the CASSCF level, which implies that the asynchronicity of TS1 is much less than that at the CASSCF level so are the correlation points and the asynchronicity of TS2. The TS of B3LYP resembled TS2, whereas those of M06-2X and LC-BLYP resembled TS1 that has a lower barrier at the MRPT2 level.

Tautomerization energies, barrier heights, and dipole moments for 7AI-CH₃OH and 7AI-(CH₃OH)₂ calculated at the TDDFT levels are listed in Table 6. The TDDFT levels predicted ΔE_T values in better agreement with the MRPT2 values than with the CASSCF without the dynamic electron correlation. However, the ΔV^\ddagger values highly depend on the size of the basis sets. For 7AI-CH₃OH, the ZPE-corrected ΔV^\ddagger values at most TDDFT levels with the 6-31G(d,p) basis set agreed well with the MRPT2 values using the same basis sets. Using the larger basis set, however, increased these values in opposition to the MRPT2 results. The bond lengths listed in Table 4 revealed that the asynchronicity of TS was increased by using larger basis sets, which produced better agreement with the CASSCF structures. However, the calculated ΔV^\ddagger values with larger basis sets were actually worse.

For 7AI-(CH₃OH)₂, we were unable to find two TSs at the TDDFT levels using the 6-31G(d,p) basis set. Interestingly, the ZPE-corrected ΔV^\ddagger values were near zero using the 6-31G(d,p) basis set and increased by using larger basis sets, in opposition to the MRPT2 results. Only two DFT methods, namely, CAM-B3LYP/6-311+G(d,p) and WB97XD/6-311+G(d,p), predicted two TSs (TS1 and TS2), whose ZPE-corrected ΔV^\ddagger values were nearly the same. The CAM-B3LYP level generated about 1 kcal/mol lower energy barriers than that of the WB97XD level. Although the M06-2X/6-311+G(d,p) level failed to locate two TSs, it produced a better ZPE-corrected ΔV^\ddagger value than the above two methods, compared with the corresponding MRPT2 value of TS1, which is probably due to the TS structure being similar to TS1, as described above.

The ZPE-corrected barrier heights of 7AI-CH₃OH and 7AI-(CH₃OH)₂ at the TDDFT/6-311+G(d,p) levels were 3.68–5.53 kcal/mol and –0.76–1.42 kcal/mol, respectively, in the gas phase. However, solvation increased the barriers by about 2–3 kcal/mol, whereas the barriers at the MRPT2 levels were reduced upon solvation. Such opposite solvent effects on the barrier heights can be explained by the dipole moments listed in Tables 3 and 6. The larger dipole moments originated from the geometric change upon solvation to increase the ionic character of the reactant and transition states in a polar solvent. Consequently, species with larger dipole moments are likely to be more stabilized in a polar solvent. At the CASSCF level, the dipole moments of TSs are greater than those of the reactants for both 7AI-CH₃OH and 7AI-(CH₃OH)₂ (Table 3), which lowers the barrier heights in solution. However, at the TDDFT levels for 7AI-CH₃OH, the dipole moments of TS were smaller than those of the reactant (Table 6), which led to larger barrier heights. Such problematic prediction of dipole moments at the TDDFT levels may originate from the incorrect estimation of the excited-state charge densities, particularly at the TS. The TDDFT barriers for 7AI-(CH₃OH)₂ in solution became larger than those in the gas phase, although the dipole moments of TS were slightly larger than those of reactant, which may require further study.

4. CONCLUSIONS

In the present work, systematic studies of the excited-state proton transfer reactions in methanol were performed on 7AI-(CH₃OH)_n (*n* = 1, 2) complexes using TDDFT and CASSCF methods. The energetics of the excited-state tautomerization depend on the dynamic electron correlation and the size of the basis sets. For the 7AI-(CH₃OH)₂ complex, CASSCF levels predicted two concerted but asynchronous paths of ESTPT; one where the proton moved first from the pyrrole ring of 7AI to methanol and the other where the methanol proton moved first to the pyridine ring. No obvious difference was found between the barrier heights of the two paths when not considering the dynamic electron correlation. However, the MRPT2 correction clearly showed that the former path was much preferable to the latter.

The MRPT2 barrier of ESDPT in 7AI-CH₃OH was 2.8 kcal/mol, which is consistent with the experimental results that the excited-state tautomerization was not observed in the gas phase but only in solution. Additionally, the 7AI-(CH₃OH)₂ MRPT2 barrier was smaller than the activation energy of solvent reorganization, so the ESTPT is not rate-limiting. Because the amount of ground-state 7AI-(CH₃OH)₂ is very small in methanol, the tautomerization by the ESTPT in 7AI-(CH₃OH)₂ might not be important.

The MRPT2 barrier of deuterium transfer in 7AI-CH₃OH is 3.81 kcal/mol (1.03 kcal/mol larger than the proton transfer), which leads to the predicted H/D KIE of 5.87. The ΔV^\ddagger value of deuterium transfer is larger than the activation energy of solvent reorganization; therefore, the intrinsic deuterium transfer is rate-limiting, but the proton transfer must compete with solvent reorganization. In the 7AI-(CH₃OH)₂ complex, the ΔV^\ddagger value of deuterium transfer is still smaller than the activation energy of methanol viscosity.

All TDDFT methods slightly underestimated tautomerization energies compared with the MRPT2 values. No significant benefits, in terms of either structural or energetic prediction, were found using the DFT methods with long-range correction

or empirical dispersion. At all TDDFT levels used in this study, the TS structures and barrier heights greatly depend on the basis set and the solvent effect. Only two methods, WB97XD and CAM-B3LYP, predicted two TSs for two asynchronous paths in the 7AI-(CH₃OH)₂ complex, although their barrier heights had nearly the same energies, unlike the MRPT2 results. The solvation increased the TDDFT barrier heights, which is attributed to the unreasonable dipole moments in the excited-state.

AUTHOR INFORMATION

Corresponding Author

*E-mail: yhkim@khu.ac.kr.

ACKNOWLEDGMENT

This research was supported in part by the Basic Science Research Program through the National Research Foundation of Korea (NRF) funded by the Ministry of Education, Science, and Technology (grant number 2010-0012990). We are pleased to acknowledge the support of the Center for Academic Computing at Kyung Hee University for the computing resources. We thank Professor Donald G. Truhlar, Department of Chemistry, University of Minnesota, for the MN-GSM and MN-GFM programs.

REFERENCES

- (1) Löwdin, P. O. *Rev. Mod. Phys.* **1963**, *35*, 724.
- (2) Löwdin, P. O. *Adv. Quantum Chem.* **1966**, *2*, 213.
- (3) Dąbkowska, I.; Rak, J.; Gutowski, M. *Eur. Phys. J.* **2005**, *35*, 429.
- (4) Gu, J.; Wang, J.; Rak, J.; Leszczynski, J. *Angew. Chem., Int. Ed.* **2009**, *46*, 3479.
- (5) Guallar, V.; Douhal, A.; Moreno, M.; Lluch, J. M. *J. Phys. Chem. A* **1999**, *103*, 6251.
- (6) McMorro, D.; Aartsma, T. *Chem. Phys. Lett.* **1986**, *125*, 581.
- (7) Chou, P. T.; Martinez, M. L.; Cooper, W. C.; Collins, S. T.; McMorro, D. P.; Kasha, M. *J. Phys. Chem.* **1992**, *96*, 5203.
- (8) Chapman, C. F.; Maroncelli, M. *J. Phys. Chem.* **1992**, *96*, 8430.
- (9) Sakota, K.; Komoto, Y.; Nakagaki, M.; Ishikawa, W.; Sekiya, H. *Chem. Phys. Lett.* **2007**, *435*, 1.
- (10) Sakota, K.; Inoue, N.; Komoto, Y.; Sekiya, H. *J. Phys. Chem. A* **2007**, *111*, 4596.
- (11) Sakota, K.; Komure, N.; Ishikawa, W.; Sekiya, H. *J. Chem. Phys.* **2009**, *130*, 224307.
- (12) Folmer, D. E.; Wisniewski, E. S.; Stairs, J. R.; Castleman, A. W., Jr. *J. Phys. Chem. A* **2000**, *104*, 10545.
- (13) Nakajima, A.; Hirano, M.; Hasumi, R.; Kaya, K.; Watanabe, H.; Carter, C.; Williamson, J. M.; Miller, T. A. *J. Phys. Chem.* **1997**, *101*, 392.
- (14) Yokoyama, H.; Watanabe, H.; Omi, T.; Ishiuchi, S.; Fujii, M. *J. Phys. Chem. A* **2001**, *105*, 9366.
- (15) Hara, A.; Sakota, K.; Sekiya, H. *Chem. Phys. Lett.* **2005**, *407*, 30.
- (16) Kwon, O. H.; Lee, Y. S.; Park, H. J.; Kim, Y. K.; Jang, D. J. *Angew. Chem., Int. Ed.* **2004**, *43*, 5792.
- (17) Lill, M. A.; Helms, V. *Proc. Natl. Acad. Sci. U.S.A.* **2002**, *99*, 2778.
- (18) Kasha, M. *J. Chem. Soc., Faraday Trans. II* **1986**, *82*, 2379.
- (19) Waluk, J. *Acc. Chem. Res.* **2003**, *36*, 832.
- (20) Tolbert, R. M.; Solntsev, K. M. *Acc. Chem. Res.* **2002**, *35*, 19.
- (21) de Grotthus, C. J. T. *Ann. Chim.* **1806**, *58*, 54.
- (22) Lodish, H.; Berk, A.; Matsudaira, P.; Kaiser, C. A.; Krieger, M.; Scott, M. P.; Zipurski, L.; Darnell, J. W. H. *Molecular Cell Biology*; Freeman & Co.: New York, 2004.
- (23) Chaban, G. M.; Gordon, M. S. *J. Phys. Chem. A* **1999**, *103*, 185.
- (24) Duong, M. P. T.; Kim, Y. H. *J. Phys. Chem. A* **2010**, *114*, 3403.
- (25) Duong, M. P. T.; Park, K. S.; Kim, Y. H. *J. Photochem. Photobiol., A* **2010**, *214*, 100.

- (26) Kina, D.; Nakayama, A.; Noro, T.; Taketsugu, T.; Gordon, M. S. *J. Phys. Chem. A* **2008**, *112*, 9675.
- (27) Sakota, K.; Jouvet, C.; Dedonder, C.; Fujii, M.; Sekiya, H. *J. Phys. Chem. A* **2010**, *114*, 11161.
- (28) Fang, H.; Kim, Y. H. *J. Chem. Theory Comput.* **2011**, *7*, 642.
- (29) Moog, R. S.; Maroncelli, M. *J. Phys. Chem.* **1991**, *95*, 10359.
- (30) Chen, Y.; Gai, F.; Petrich, J. W. *J. Am. Chem. Soc.* **1993**, *115*, 10158.
- (31) Frisch, M. J.; Trucks, G. W.; Schlegel, H. B.; Scuseria, G. E.; Robb, M. A.; Cheeseman, J. R.; Scalmani, G.; Barone, V.; Mennucci, B.; Petersson, G. A.; Nakatsuji, H.; Caricato, M.; Li, X.; Hratchian, H. P.; Izmaylov, A. F.; Bloino, J.; Zheng, G.; Sonnenberg, J. L.; Hada, M.; Ehara, M.; Toyota, K.; Fukuda, R.; Hasegawa, J.; Ishida, M.; Nakajima, T.; Honda, Y.; Kitao, O.; Nakai, H.; Vreven, T.; Montgomery, J. A., Jr.; Peralta, J. E.; Ogliaro, F.; Bearpark, M.; Heyd, J. J.; Brothers, E.; Kudin, K. N.; Staroverov, V. N.; Kobayashi, R.; Normand, J.; Raghavachari, K.; Rendell, A.; Burant, J. C.; Iyengar, S. S.; Tomasi, J.; Cossi, M.; Rega, N.; Millam, J. M.; Klene, M.; Knox, J. E.; Cross, J. B.; Bakken, V.; Adamo, C.; Jaramillo, J.; Gomperts, R.; Stratmann, R. E.; Yazyev, O.; Austin, A. J.; Cammi, R.; Pomelli, C.; Ochterski, J. W.; Martin, R. L.; Morokuma, K.; Zakrzewski, V. G.; Voth, G. A.; Salvador, P.; Dannenberg, J. J.; Dapprich, S.; Daniels, A. D.; Farkas, O.; Foresman, J. B.; Ortiz, J. V.; Cioslowski, J.; Fox, D. J. *Gaussian 09*, revision A.01; Gaussian, Inc.: Wallingford, CT, 2009.
- (32) Schmidt, M. W.; Baldridge, K. K.; Boatz, J. A.; Elbert, S. T.; Gordon, M. S.; Jensen, J. H.; Koseki, S.; Matsunaga, N.; Nguyen, K. A.; Su, S. J.; et al. *J. Comput. Chem.* **1993**, *14*, 1347.
- (33) Furche, F.; Ahlrichs, R. *J. Chem. Phys.* **2002**, *117*, 7433.
- (34) Becke, A. D. *J. Chem. Phys.* **1993**, *98*, 5648.
- (35) Yanai, T.; Tew, D.; Handy, N. *Chem. Phys. Lett.* **2004**, *393*, 51.
- (36) Iikura, H.; Tsuneda, T.; Yanai, T.; Hirao, K. *J. Chem. Phys.* **2001**, *115*, 3540.
- (37) Zhao, Y.; Truhlar, D. G. *Theor. Chem. Acc.* **2008**, *120*, 215.
- (38) Cancès, E.; Mennucci, B.; Tomasi, J. *J. Chem. Phys.* **1997**, *107*, 3032.
- (39) Cossi, M.; Barone, V.; Mennucci, B.; Tomasi, J. *Chem. Phys. Lett.* **1998**, *286*, 253.
- (40) Mennucci, B.; Tomasi, J. *J. Chem. Phys.* **1997**, *106*, 5151.
- (41) Olson, R. M.; Marenich, A. V.; Cramer, C. J.; Truhlar, D. G. *J. Chem. Theory Comput.* **2007**, *3*, 2046.
- (42) Frisch, M. J.; Trucks, G. W.; Schlegel, H. B.; Scuseria, G. E.; Robb, M. A.; Cheeseman, J. R.; Montgomery, J. A., Jr.; Vreven, T.; Kudin, K. N.; Burant, J. C.; Millam, J. M.; Iyengar, S. S.; Tomasi, J.; Barone, V.; Mennucci, B.; Cossi, M.; Scalmani, G.; Rega, N.; Petersson, G. A.; Nakatsuji, H.; Hada, M.; Ehara, M.; Toyota, K.; Fukuda, R.; Hasegawa, J.; Ishida, M.; Nakajima, T.; Honda, Y.; Kitao, O.; Nakai, H.; Klene, M.; Li, X.; Knox, J. E.; Hratchian, H. P.; Cross, J. B.; Bakken, V.; Adamo, C.; Jaramillo, J.; Gomperts, R.; Stratmann, R. E.; Yazyev, O.; Austin, A. J.; Cammi, R.; Pomelli, C.; Ochterski, J. W.; Ayala, P. Y.; Morokuma, K.; Voth, G. A.; Salvador, P.; Dannenberg, J. J.; Zakrzewski, V. G.; Dapprich, S.; Daniels, A. D.; Strain, M. C.; Farkas, O.; Malick, D. K.; Rabuck, A. D.; Raghavachari, K.; Foresman, J. B.; Ortiz, J. V.; Cui, Q.; Baboul, A. G.; Clifford, S.; Cioslowski, J.; Stefanov, B. B.; Liu, G.; Liashenko, A.; Piskorz, P.; Komaromi, I.; Martin, R. L.; Fox, D. J.; Keith, T.; Al-Laham, M. A.; Peng, C. Y.; Nanayakkara, A.; Challacombe, M.; Gill, P. M. W.; Johnson, B.; Chen, W.; Wong, M. W.; Gonzalez, C.; Pople, J. A. *Gaussian 03*, revision E.01; Gaussian, Inc.: Wallingford, CT, 2003.
- (43) Olson, R. M.; Marenich, A. V.; Chamberlin, A. C.; Kelly, C. P.; Thompson, J. D.; Xidos, J. D.; Li, J.; Hawkins, G. D.; Winget, P. D.; Zhu, T. D.; et al. *MN-GSM*, version 2008; University of Minnesota: Minneapolis, MN, 2008.
- (44) Zhao, Y.; Truhlar, D. G. *MN-GFM*, version 3.0; University of Minnesota: Minneapolis, MN, 2008.
- (45) Boys, S. F.; Bernardi, F. *Mol. Phys.* **1970**, *19*, 553.
- (46) Taylor, C. A.; El-Bayoumi, M. A.; Kasha, M. *Proc. Natl. Acad. Sci. U.S.A.* **1969**, *63*, 253.
- (47) Kojnenberg, J.; Huizer, A. H.; Varma, C. A. G. O. *J. Chem. Soc., Faraday Trans. II* **1988**, *84*, 1163.
- (48) Smirnov, A. V.; English, D. S.; Rich, R. L.; Lane, J.; Teyton, L.; Schwabacher, A. W.; Luo, S.; Thornburg, R. W.; Petrich, J. W. *J. Phys. Chem. B* **1997**, *101*, 2758.
- (49) Zhao, Y.; Truhlar, D. G. *J. Chem. Theory Comput.* **2008**, *4*, 1849.
- (50) Zheng, J.; Zhao, Y.; Truhlar, D. G. *J. Chem. Theory Comput.* **2009**, *5*, 808.
- (51) Marenich, A. V.; Olson, R. M.; Kelly, C. P.; Cramer, C. J.; Truhlar, D. G. *J. Chem. Theory Comput.* **2007**, *3*, 2011.
- (52) Sakota, K.; Kageura, Y.; Sekiya, H. *J. Chem. Phys.* **2008**, *129*, 054303.
- (53) Kyrychenko, A.; Stepanenko, Y.; Waluk, J. *J. Phys. Chem. A* **2000**, *104*, 9542.
- (54) Mente, S.; Maroncelli, M. *J. Phys. Chem. A* **1998**, *102*, 3860.
- (55) Limbach, H. H.; Pietrzak, M.; Benedict, H.; Tolstoy, P. M.; Golubev, N. S.; Denisov, G. S. *J. Mol. Struct.* **2004**, *706*, 115.
- (56) Limbach, H. H.; Lopez, J. M.; Kohen, A. *Philos. Trans. R. Soc., B* **2006**, *361*, 1399.
- (57) Limbach, H. H. In *Hydrogen-Transfer Reactions*; Schowen, R. L., Klinman, J. P., Hynes, J. T., Limbach, H. H., Eds.; Wiley: Weinheim, Germany, 2007; Chapter 6, pp 135–221.
- (58) Garrett, B. C.; Truhlar, D. G. *J. Am. Chem. Soc.* **1979**, *101*, 4534–4548.
- (59) Johnston, H. S. *Gas Phase Reaction Rate Theory*; Ronald Press: New York, 1966; pp 1–362.